Supplementary Information for

The aryl hydrocarbon receptor instructs the immunomodulatory profile of a subset of Clec4a4^{+} eosinophils unique to the small intestine

Wei-Le Wang[1*], Jun Kasamatsu[1, 2*], Satoru Joshita[1, 3*], Susan Gilfillan[1], Blanda Di Luccia[1], Santosh Panda[1], Do-Hyun Kim[1], Pritesh Desai[4], Jennifer K. Bando[1,5], Stanley Ching-Cheng Huang[1,6], Kentaro Yomogida[1], Hitomi Hoshino[7], Mana Fukushima[7], Elizabeth A. Jacobsen[8], Steven Van Dyken[1], Christiane Ruedl[9], Marina Cella[1], Marco Colonna[1]

Correspondence: Marco Colonna

Email: mcolonna@wustl.edu

This PDF file includes Materials and Methods, and Figures S1 to S5

***SI Appendix, Materials and Methods*.**

Mice and treatments

All mice were bred and maintained at a specific pathogen-free facility at Washington University School of Medicine in Saint Louis, MO, under protocols reviewed and approved by the Washington University Animal Studies Committee. Sex- and age-matched littermates were used for each experiment. *Ahr*$^{-/-}$ mice, mice with loxP-flanked Ahr alleles were breed as described previously (1). C57BL/6-background CD45.1 were purchased from Jackson Laboratory. Clec4a4-diphtheria toxin receptor (DTR) mice were previously described (2). *Eo*^{Cre} mice were kindly provided by Elizabeth Jacobsen (Division of Pulmonary Medicine, Mayo Clinic Arizona, Scottsdale, AZ). Germ-free (GF) mice were housed in tightly controlled and monitored isolators to prevent bacterial colonization. Microbiota transfers using *L. reuteri* 100-23 and *L. reuteri* ΔArAT were performed as previously described (3). Purified diet (TD.97184) and diet supplemented with indole-3-carbinol (2000 ppm, TD.180703) were purchased from Envigo and fed to mice as described in the main text. A high-fat diet (D12492) with 60 kcal% fat was purchased from Research Diet and mice were fed for one week.

Generation of Clec4a4-mCherry knock-in mice

Clec4a4-mCherry knock-in mice were generated by insertional mutation of a gene trap cassette into the intron downstream of exon 3 of the *Clec4a4* gene using homologous recombination in C57BL/6J embryonic stem cells. The cassette consisted of a splice acceptor, a T2A sequence followed by human histone H2B fused to the mCherry reporter and a poly A signal (**see Fig. 1A**). The translational stop codon of the coding sequence for mCherry was retained. For selection, puromycin N-acetyltransferase driven by a PGK promoter was inserted adjacent 3' to H2BmCherry. Ultimately, the mCherry transcript lacked the functional C-type lectin domain encoded by exon 4 to exon 6. Correctly targeted homologous recombinant ES clones were identified by Southern blot and used to generate chimeric mice that transmitted the targeted allele to their offspring.

Mixed bone marrow chimeras

To generate mixed-bone marrow (BM) chimeric mice, tibial and femur BM cells from 6-weeks-old *Ahr*$^{-/-}$ (CD45.2), C57BL/6 mice (CD45.1/2) were harvested. After removal of red blood cells, BM cells were counted and mixed at a 1:1 ratio then injected into lethally irradiated (1,000 rad) congenic C57BL/6 mice (CD45.1). 3×10^6 cells of each genotype were injected *i.v.* 24 h after irradiation. BM chimeras were analyzed 8 weeks after reconstitution.

Cell preparation

Single cell suspension from various tissue were prepared following protocols previously described (4). Briefly, small intestines were flushed, and Peyer's patches were removed. To remove Intraepithelial lymphocytes (IELs), tissues were incubated in 20 mL of HBSS buffer with 10% FCS, 15 mM EDTA and 15 mM HEPES at room temperature for 20 min under agitation. After IEL removal, LP cells were extracted by digesting tissue in complete RPMI medium containing 10% FCS and 1 mg ml^{-1} Collagenase IV (Sigma-Aldrich) at 37°C for 1h under agitation. The dissected lung and liver were cut into small pieces and

incubated in digestion buffer containing RPMI medium with 10% FCS and 1 mg ml^{-1} Collagenase IV (Sigma-Aldrich) at 37°C for 1h under agitation. Digested single-cell suspensions were filtered through a 100-micron mesh and subjected to density gradients using 40% and 70% Percoll. Adipose tissue and BM samples were pulverized for isolation of lymphocytes.

Antibodies and flow cytometry

Fc receptors were blocked before staining with supernatant from hybridoma cells producing monoclonal antibodies to CD32 (HB-197, ATCC). For intra-cellular cytokine staining, a BD Bioscience Fixation/Permeabilization Solution kit was used according to the manufacturer's instructions. Data were acquired with a BD FACSCanto II (BD Biosciences) or LSRFortessa (BD Biosciences) and analyzed using FlowJo (TreeStar). The following antibodies were used: anti-Clec4a4 (33D1; BioLegend), anti-CD45 (30-F11; eBioscience), anti-CD11b (M1/70; eBioscience), anti-Siglec-F (E50-2440; BD Biosciences), anti-CD3ε (145-2C11; BioLegend), anti-CD4 (GK1.5; eBioscience), anti-MHC class II (I-A/I-E) (M5/114.15.2; eBioscience), anti-CD45.1 (A20; eBioscience), anti-CD45.2 (104; eBioscience), anti-CD11c (N418; BioLegend), anti-CCR3 (J073E5; BioLegend), anti-CD8α (53-6.7; eBioscience), anti-F4/80 (BM8; eBioscience), anti-CD64 (X54-5/7.1; BioLegend), anti-CD22 (OX-97; BioLegend), anti-CD68 (FA-11; BioLegend), anti-PECAM-1/CD31 (MEC13.3; BioLegend), anti-LPAM1 (DATK32; BioLegend), anti-CD62L (MEL-14; eBioscience), anti-CD101 (Moushi101; eBioscience).

Immunohistochemistry

Tissue staining was performed as previously described (5). Small intestines derived from $Clec4a4^{mCherry/+}$ mice were fixed with 4% PFA (Electron Microscopy Sciences) in PBS for 2 h, and then left in PBS overnight. Next, tissues were incubated in 30% sucrose for 2 h before being frozen in OCT compound (Sakura). Frozen tissue blocks were sectioned at 8 microns in thickness using a Leica CM3050-S cryostat. Sections were incubated with 3% H_2O_2, 0.1% NaN3 in PBS for 45 min to quench endogenous peroxidase, and then blocked with rat anti-mouse CD16/CD32, 1% mouse serum and 1% rat serum for 1 h. Sections were stained with rat anti-mouse Siglec-F (E50-2440; BD Biosciences). DAPI was added to sections for 5 min to visualize nuclei.

RNA isolation and RT-qPCR analysis

RNA was isolated using the RNeasy Micro Kit (Qiagen) and RNeasy Mini Kit (Qiagen) for microarray analysis and RT-qPCR analysis, respectively. Purified RNA was reverse transcribed with oligo(dT)20 primer using the SuperScript III first strand synthesis system (Invitrogen). Resultant cDNA was diluted in nuclease-free water and used for real-time PCR using iTaq Universal SYBR Green Supermix (Bio-Rad) on a StepOnePlus (Applied Biosystems). The expressions of target genes were calculated and normalized to that of the control gene, *Gapdh*, using the $2^{-\Delta\Delta CT}$ method. The primer pairs for qRT-PCR were as follows (6-8): *Gapdh* forward-GCCTGGAGAAACCTGCCA; *Gapdh* reverse-CCCTCAGATGCCTGCTTCA; *Ahr* forward-GACAGTTTTCCGGCTTCTTG; *Ahr* reverse-CGCTTCTGTAAATGCTCTCGT; *Cyp1b1* forward-CTTCGCCTCTTTCCGTGTG; and *Cyp1b1* reverse-GTGACCGAACGCCAGACTG.

Microarray analysis

Eosinophil subsets were FACS sorted from the siLP of Clec4a4-mCherry knock-in mice to identify Clec4a4^{+} and Clec4a4^{-} eosinophils. In addition, eosinophils from WT and *Ahr*$^{-/-}$ mice were sorted to identify AHR-dependent and AHR-independent genes. Sorting gates were applied on CD45^{+} Siglec-F^{+} CD11b^{+} MHC class II^{-} SSC^{high} mCherry^{+} or mCherry^{-} cells. Microarray analysis was performed as previously described (9). RNA was amplified with Ovation PicoSL (NuGEN) and the product was hybridized to Affymetrix Mouse Gene 1.0 ST arrays. Analysis was carried out as previously described (10). Briefly, CEL files were normalized with AffySTExpressionFileCreator modules of GenePattern using robust multi-array average (RMA). Differences in gene expression were identified using the Multiplot Studio function of GenePattern17 (Broad Institute) from a filtered subset of genes with coefficients of variation of less than 0.1 in all samples and expression of at least 120 relative units in 1 subset by the class mean function. Gene expression was considered 'unique' or 'shared' if expression was greater than 2-fold and the p-value was < 0.05 (Student's t-test) in the indicated subset. Graphs were produced by Multiplot Studio and MORPHEUS software (https://software.broadinstitute.org/morpheus/).

Gene Set Enrichment Analysis

Differentially expressed genes derived from microarray analysis were subjected to GSEA analysis. GSEA analysis (http://software.broadinstitute.org/gsea/index.jsp) (11) was performed with the RMA normalized values from the 25,544 expressed genes. Hallmark gene sets from Molecular Signatures Database (MSigDB) v7.1 were evaluated for enrichment.

Induction of food allergy by OVA

Mice were sensitized at day 0 and day 14 with 50 micrograms of Ova (Sigma cat: A-5503) and 1 mg of alum (Sigma cat: A-7210) intraperitoneally. Starting at day 28 mice were challenged with 50 mg of Ova by oral gavage every 3 days for 14 times. At day 70 mice were weighted and sacrificed.

H. polygyrus infection

H. polygyrus third-stage larvae (L3) were prepared as earlier described (12). Mice were orally gavaged with 200 L3 or water (mock) with a 20-gauge ball-tipped gavage needle. The animals were sacrificed on day 3, 8, and 14 of infection for assessment of immune cells. *H. polygyrus* egg counts were performed on fecal pellets using a McMaster 2 cell counter (Hawksley) on days 10, 12, 14, 16, and 18 following infection.

N. brasiliensis infection

N. brasiliensis third-stage larvae (L3) were prepared as earlier described (13). Mice were subcutaneously injected with 500 L3 via an 18-gauge needle. The animals were sacrificed on day 6 post-infection for assessment of immune cells. To enumerate the number of adult *N. brasiliensis*, small intestines were collected, placed in PBS and incubated at 37°C for 1 hour. Worm counts were performed using a dissection microscope.

Quantification and statistical analysis

Data were analyzed with either *t*-tests or one-way ANOVA and Tukey post-hoc tests by GraphPad Prism 9.0.0 software (GraphPad Software. San Diego, CA). Each point in the graphs indicated biological replicates, except where indicated in figure legends. All statistics are presented in figure legends.

References for SI Appendix Materials and Methods

1. J. S. Lee *et al.*, AHR drives the development of gut ILC22 cells and postnatal lymphoid tissues via pathways dependent on and independent of Notch. *Nat Immunol* **13**, 144-151 (2011).
2. A. R. Muzaki *et al.*, Intestinal CD103(+)CD11b(-) dendritic cells restrain colitis via IFN-γ-induced anti-inflammatory response in epithelial cells. *Mucosal Immunol* **9**, 336-351 (2016).
3. L. Cervantes-Barragan *et al.*, *Lactobacillus reuteri* induces gut intraepithelial $CD4^+$ $CD8\alpha\alpha^+$ T cells. *Science* **357**, 806-810 (2017).
4. J. K. Bando *et al.*, The Tumor Necrosis Factor Superfamily Member RANKL Suppresses Effector Cytokine Production in Group 3 Innate Lymphoid Cells. *Immunity* **48**, 1208-1219.e1204 (2018).
5. J. K. Bando, H. E. Liang, R. M. Locksley. Identification and distribution of developing innate lymphoid cells in the fetal mouse intestine. *Nat Immunol* 1**6**, 153-160 (2015).
6. J. Kasamatsu *et al.*, INAM plays a critical role in IFN-γ production by NK cells interacting with polyinosinic-polycytidylic acid-stimulated accessory cells. *J Immunol* **193**, 5199-5207 (2014).
7. J. Tigges *et al.*, Aryl hydrocarbon receptor repressor (AhRR) function revisited: repression of CYP1 activity in human skin fibroblasts is not related to AhRR expression. *J Invest Dermatol* **133**, 87-96 (2013).
8. V. Laugel-Haushalter *et al.*, Molars and incisors: show your microarray IDs. *BMC Res Notes* **6**, 113 (2013).
9. M. L. Robinette *et al.*, IL-15 sustains IL-7R-independent ILC2 and ILC3 development. *Nat Commun* **8**, 14601 (2017).
10. M. L. Robinette *et al.*, Transcriptional programs define molecular characteristics of innate lymphoid cell classes and subsets. *Nat Immunol*, **16**, 306-317 (2015)
11. A. Subramanian *et al.*, Gene set enrichment analysis: a knowledge-based approach for interpreting genome-wide expression profiles. *Proc Natl Acad Sci U S A* **102**, 15545-15550 (2005).
12. S. C. Huang *et al.*, Cell-intrinsic lysosomal lipolysis is essential for alternative activation of macrophages. *Nat Immunol* **15**, 846-855 (2014).
13. A. E. Price *et al.*, Systemically dispersed innate IL-13-expressing cells in type 2 immunity. *Proc Natl Acad Sci U S A* **107**, 11489-11494 (2010).

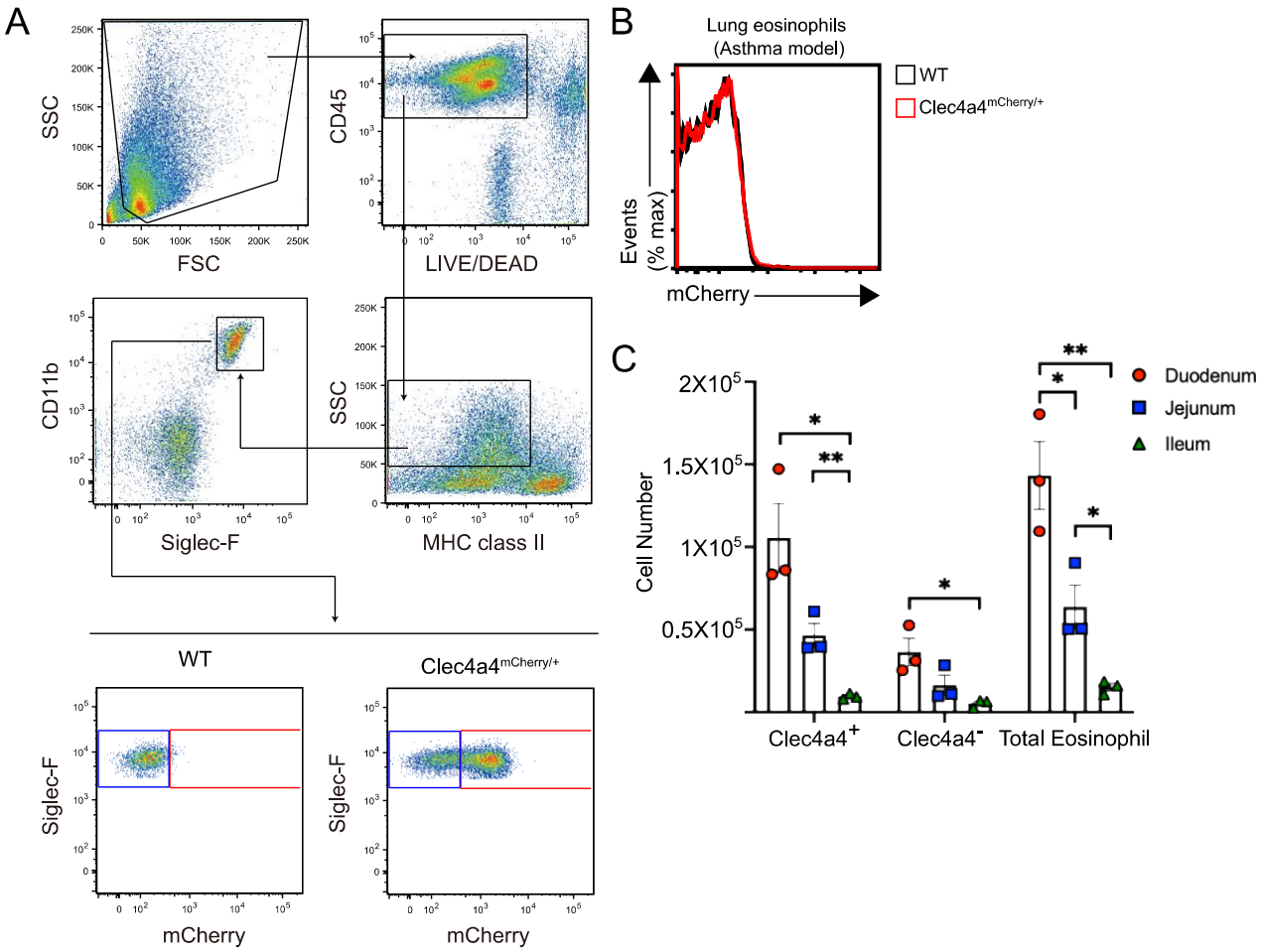

***SI Appendix*, Fig. S1. Gating strategy and characterization of Clec4a4$^+$ or mCherry$^+$ eosinophils in the lung and small intestine.** (A) Gating strategy for identification of mCherry$^+$ and mCherry$^-$ eosinophils in small intestine. A gate was applied on alive, CD45$^+$, MHCII$^{low/-}$, SSC^{high}, CD11b$^+$ and Siglec-F$^+$ cells and the two subsets of eosinophils were identified based on mCherry expression. (B) mCherry expression in lung eosinophils during house dust mite (HDM)-induced allergic airway inflammation. (C) Absolute numbers of siLP Clec4a4$^+$, Clec4a4$^-$ and total eosinophils in the duodenum, jejunum and ileum of WT mice in homeostatic conditions. Results are shown as mean ± SEM. *P* values were calculated using multiple unpaired *t* test; *, $P < 0.05$; **, $P < 0.01$.

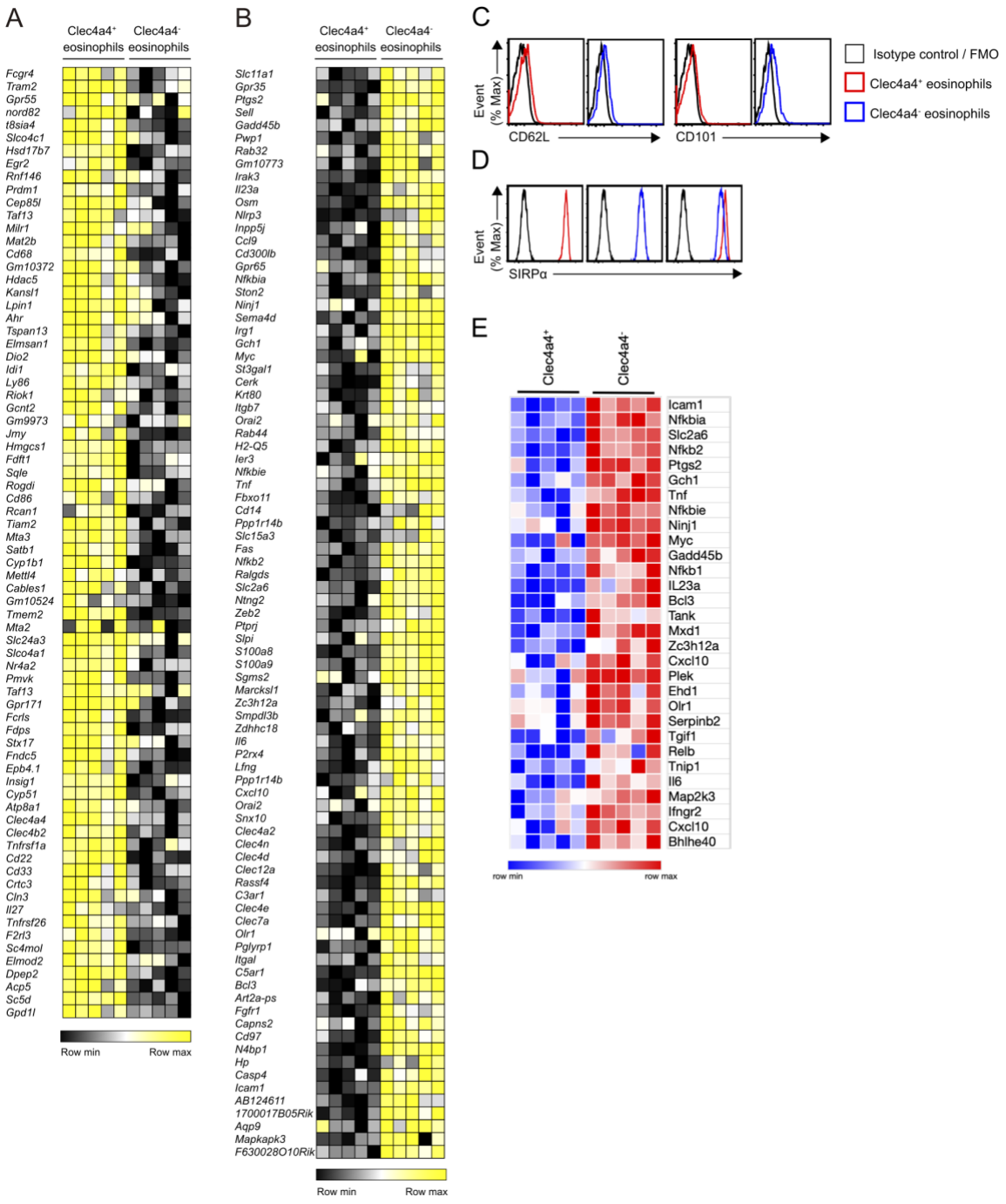

***SI Appendix*, Fig. S2. mRNA transcripts differentially expressed between Clec4a4$^+$ and Clec4a4$^-$ eosinophils.** (A) Heat map of 74 transcripts upregulated in Clec4a4$^+$ eosinophils. (B) Heat map of 85 transcripts upregulated in Clec4a4$^-$ eosinophils. (C) Expression of CD62L, CD101, and (D) SIRPα in Clec4a4$^+$ and Clec4a4$^-$ eosinophils from siLP. (E) Heat map of transcripts associated with the "TNFα signaling via NF-κB pathway" enriched in the Clec4a4$^-$ eosinophils.

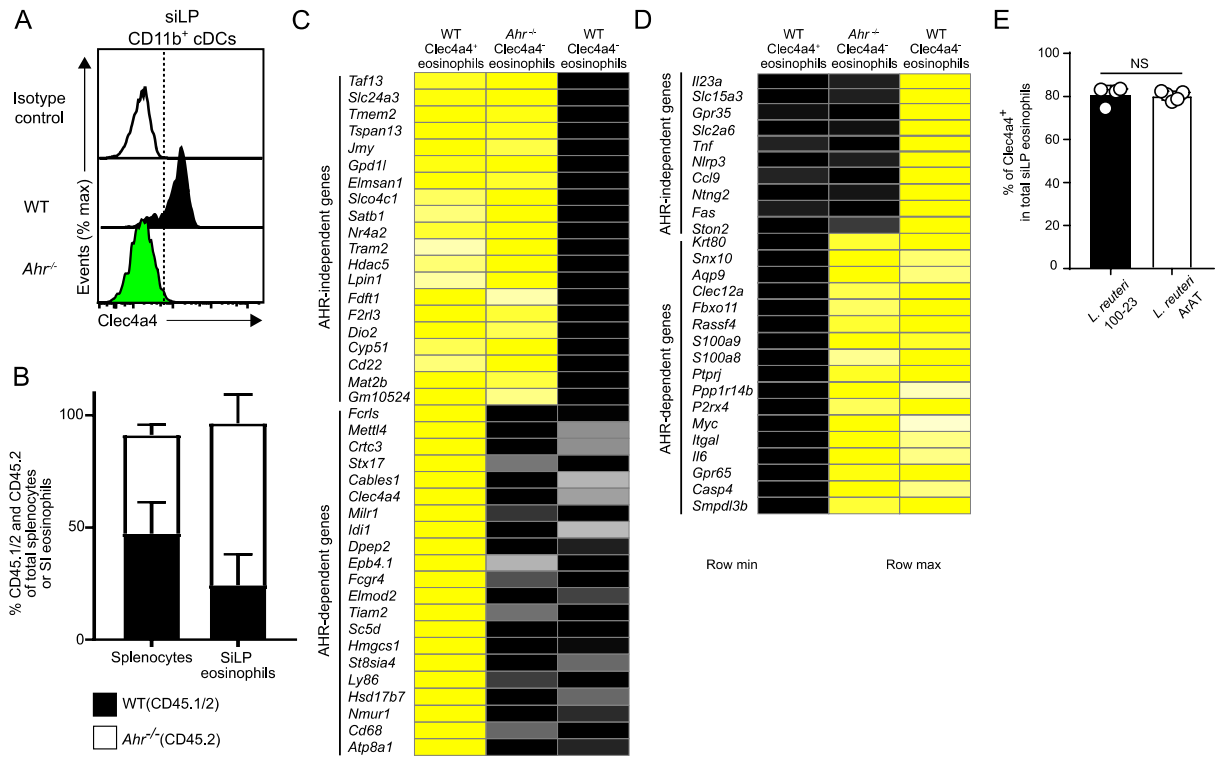

***SI Appendix*, Fig. S3. AHR-dependent and independent regulations of gene expression in Clec4a4$^+$ siLP eosinophils.** (A) Clec4a4 expression in siLP CD11b$^+$ cDCs derived from WT and *Ahr*$^{-/-}$ mice. (B) Percentages of WT (CD45.1/2) and AHR-deficient (CD45.2) cells among CD45$^+$ splenocytes and total siLP eosinophils in BM-chimeras 8 weeks after reconstitution. (C) Heat map of Clec4a4$^+$ specific transcripts from WT and *Ahr*$^{-/-}$ mice. (D) Heat map of Clec4a4$^-$ specific transcripts from WT and *Ahr*$^{-/-}$ mice. AHR dependent and independent genes are shown. Each sample was a pool of sorted WT Clec4a4$^+$, WT Clec4a4$^-$ or *Ahr*$^{-/-}$ Clec4a4$^-$ siLP eosinophils from 3 mice. (E) Frequency of intestinal Clec4a4$^+$ eosinophils in mice re-colonized with either *L. reuteri* 100-23 or *L. reuteri* ArAT (n=4, each group).

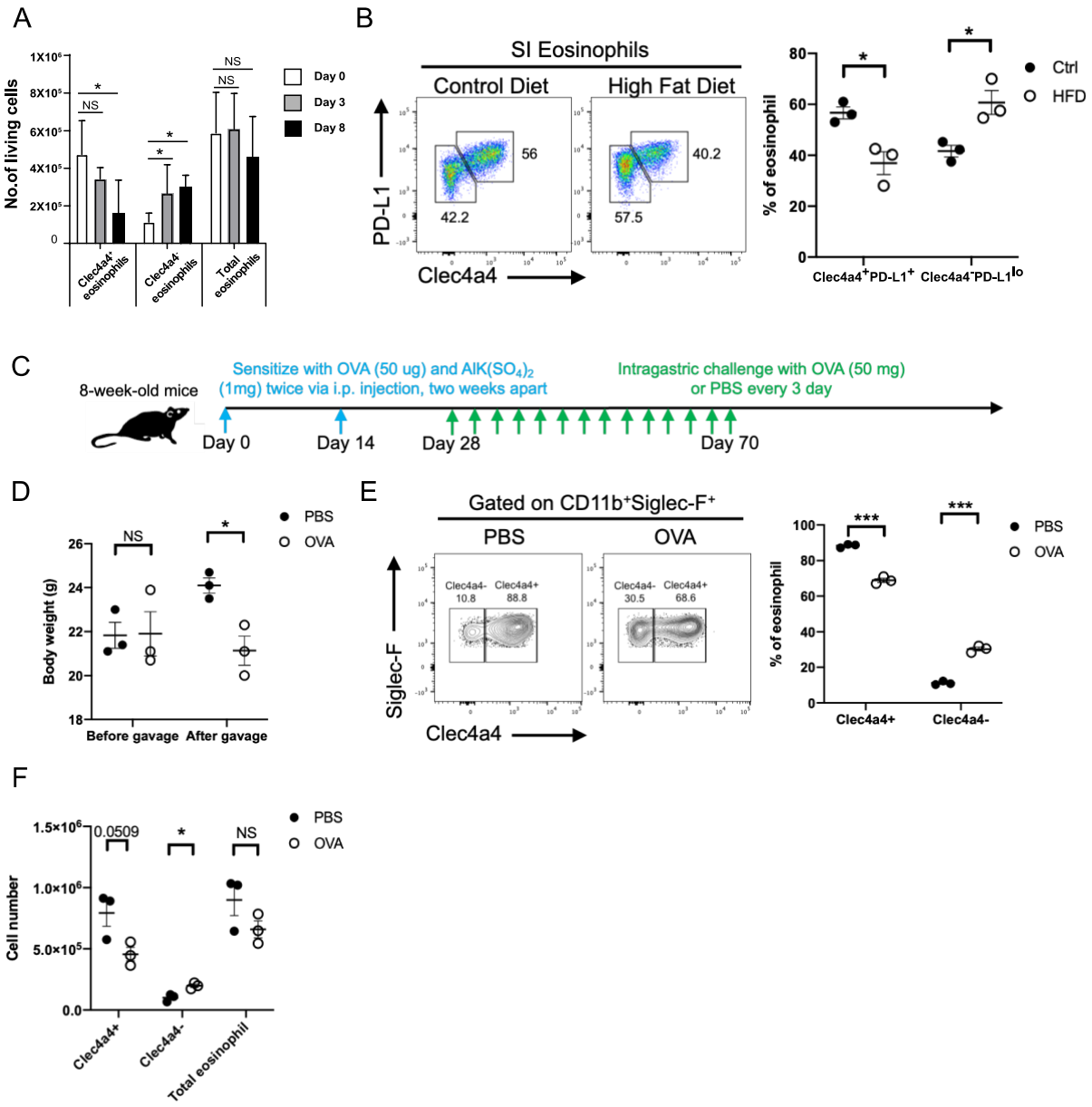

***SI Appendix*, Fig. S4. The frequency of siLP Clec4a4$^+$ eosinophil is reduced during helminth infection, high-fat diet, and food allergy.** (A) Absolute numbers of Clec4a4$^+$ and Clec4a4$^-$ eosinophils at the indicated times during *H. polygyrus* infection. (B) Left panel, expression of Clec4a4 and PD-L1 in siLP eosinophils derived from mice fed with standard or high-fat diet. Right panel, frequency of Clec4a4$^+$PD-L1$^+$ and Clec4a4$^-$PD-L1^{lo} siLP eosinophils in mice fed with standard or high-fat diet (n=3). (C) Experimental time line of food allergy induction with OVA and Alum in Balb/c mice. (D) Body weight before and after intragastric challenge with OVA. (E) Left panel, expression of Clec4a4 in siLP eosinophils in mice challenged with PBS or OVA. Right panel, frequency of Clec4a4$^+$ and Clec4a4$^-$ eosinophils in mice challenge with PBS or OVA. (F) Absolute numbers of Clec4a4$^+$ and Clec4a4$^-$ eosinophils in mice challenged with PBS or OVA. *P* values were calculated using multiple unpaired *t* test; NS, not significant; *, $P < 0.05$; ***, $P < 0.001$.

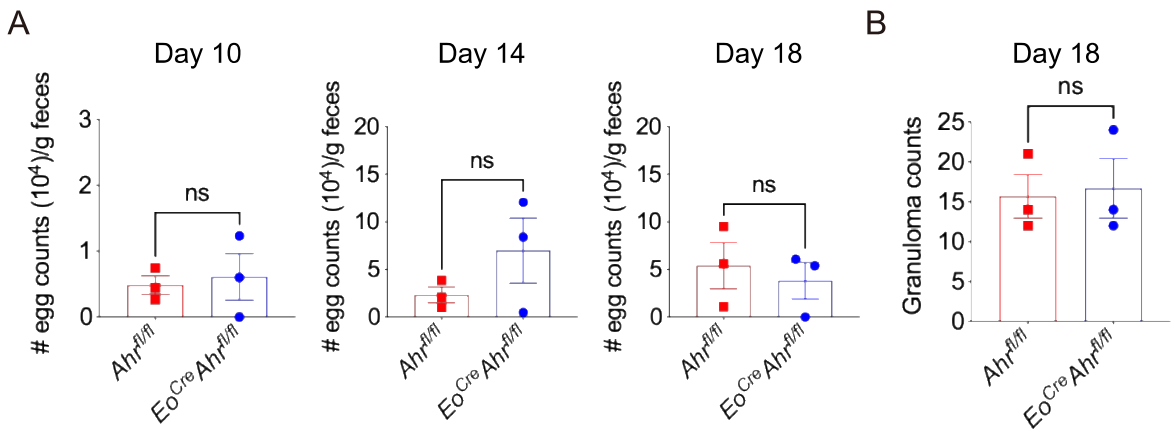

***SI Appendix*, Fig. S5. *H. polygyrus* infection of $Ahr^{fl/fl}$ and $Eo^{Cre}Ahr^{fl/fl}$ mice.** (A) Egg counts in feces of $Ahr^{fl/fl}$ and $Eo^{Cre}Ahr^{fl/fl}$ mice on day 10, 14, and 18. (B) Granuloma counts in small intestine of $Ahr^{fl/fl}$ and $Eo^{Cre}Ahr^{fl/fl}$ mice at day 18 post-infection. Results are shown as mean ± SEM. *P* values were calculated using Mann-Whitney test; NS, not significant.